ENERGY PARTITIONS IN THREE-DIMENSIONAL SIMULATIONS OF THE CHICXULUB METEOR IMPACT. G. R. Gisler[1] , R. P. Weaver[1], and M. L. Gittings[2], [1]Los Alamos National Laboratory, MS T087, Los Alamos NM 87545, [2]Science Applications International, MS T087, Los Alamos NM 87545.

Introduction: We have performed several three-dimensional simulations of the meteor impact at Chicxulub, Mexico with the Continuous Adaptive Mesh Refinement code SAGE. This impact is widely believed to be associated with the mass-extinction event at the end of the Cretaceous period and may have caused this extinction by a combination of widespread wildfires, high atmospheric opacity, atmospheric toxicity, and severe climate excursions. The worldwide distribution of shocked quartz, platinum-group elements, tektites, and soot in the K/T boundary layer can provide important diagnostics of the dynamics of the impact and the mechanisms of extinction [1]. Studies of the energy partitions among simulations at various angles of impact and projectile characteristics are useful in elucidating the relation between the impact event, the distributed evidence in the K/T boundary layer, and the extinction mechanism.

The Code: The SAGE code is a fully-compressible multiphase multifluid hydrocode using a Godunov scheme for second-order accuracy. It has been jointly developed by the Los Alamos National Laboratory and Science Applications International, is extensively tested against both analytical problems and laboratory-scale experiments, and has been additionally benchmarked against large-scale geophysical events including volcanic eruptions and tsunamis. Equations of state used in the code include a range of analytical formulations, tabular material from the Los Alamos SESAME library (modified to remove van-der-Waals loops via the Maxwell construction), and a special tabular equation for water developed by SAI to include nearly all known phase transitions. A simple elastic/ plastic strength model was used for the solid materials in the target in these calculations.

The Setup: All simulations reported here were set up with a layered target consisting of a US standard atmosphere of 78 km height and a scale height of 7 km, a water depth of 500 meters, a mixed water/solid calcite region 4.5 km thick, linearly stratified from pure water at the top to pure calcite at the bottom, a granite region 30 km thick, and a mantle region 15 km thick. This vertical stratification is indicated schematically in Figure 2 below. The projectile in all cases is a sphere of 12 km diameter, with the density and equation of state of granite, but without strength, and having a velocity of 20 km/s.. We report here on 4 such simulations having projectile trajectories of 15˚, 30˚, 45˚ and 60˚ with respect to the horizontal. All projectiles were started at an altitude of 40 km, except for the 15˚ run, in which a 20 km initial altitude was used. The computational domain is a box with horizontal dimension 256km x 256 km and vertical dimension 128 km. Outflow boundary conditions (freeze regions) are used. Our aim is to run these simulations until most of the ejected material has either achieved ballistic trajectories or been deposited locally. This generally requires two to three minutes of physical time, or several months of computational time on 512 processors. So far we have achieved this with all but the 60˚ simulation, which has only run out to 5.5 seconds past impact. These longer-time studies supplement earlier work by Pierazzo and collaborators on effects of impact angle [2].

Results: The only free energy at the start of the problem is the asteroid's kinetic energy. In Figure 1 we plot the partition of energies at 5 seconds after the asteroid's kinetic energy is reduced to 75% of its initial value. (The lines indicating internal energy are in fact the changes from initial values of internal energy for the components.) As is expected, shallow impacts deliver much less energy to the target than deep impacts do. In particular, shallow angles of impact do not excavate enough granite to account for the distribution of shocked quartz from the Chicxulub event. In fact, at an angle as low as 15˚, most of the energy of impact is retained in the fragmented and vaporized asteroid material, which mainly propagates downrange at low altitude (Figure 2). At successively greater angles of impact (Figures 3 and 4) more granite is excavated, and with more energy and greater isotropy. The dispersal of projectile material also becomes more uniform with steeper angles of impact. These results suggest that a relatively steep angle of impact (45˚ or greater) may be necessary to account for the worldwide distribution of platinum-group elements in the K/T boundary layer and also for the similarly broad distribution of shocked quartz [3]. Peak pressures at the calcite/granite interface are shown in Figure 5

In contrast, more thermal energy is injected directly into the troposphere downrange of the impact point for shallow-angle impacts, while much thermal energy escapes through the top of the atmosphere when the impact angle is steep. In a shallow-angle impact, it would therefore be expected that fires would be immediately ignited on land downrange from the impact site, while for a steep-angle impact the first fires (if any) might well be set at points very distant from the impact site, even near the antipode, by the hot re-entry of ballistically ejected material. The lack of charcoal deposits in K/T boundary sediments in North American sites [4] evidently provides an additional argument that the impact angle must not have been shallow.

A steeper impact that excavated more material from the granitic crust beneath the carbonate platform at Chicxulub, might instead have induced an environmental catastrophe by poisoning and darkening of the late-Cretaceous atmosphere.

References:

[1] Smits J. (1999) *Annu. Rev. Earth Planet.Sci.* **27**: 75-113. [2] Pierazzo E. and Melosh H. J. (2000) *Annu. Rev. Earth Planet.Sci.* **28**:141-67. [3] Croskell M. *et al.* (2002) *Geophys. Res. Lett.*, **29**, No. 20. [4] Belcher C. M. *et al.* (2005) *J. Geol. Soc. Lond.* **162,** 591-602**.**

Figures:

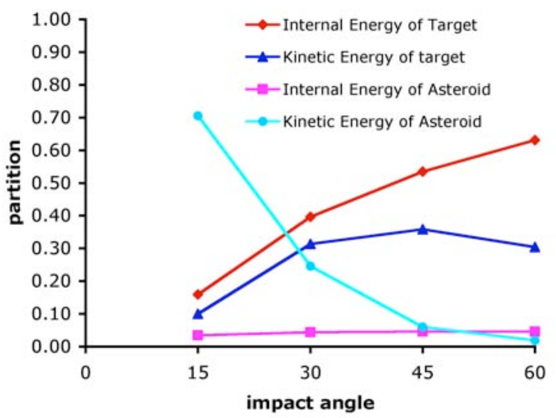

Figure 1: Partition of energies (relative to the initial asteroid kinetic energy) at 5 seconds after the time at which the projectile's kinetic energy is 75% of its initial value for the 4 runs reported here. At shallow angles of impact, most of the initial kinetic energy is retained by the asteroid, whose material skips downrange in a relatively tightly focussed stream. At angles of impact greater than about 45˚, more than 90% of the energy of impact is transmitted to relatively deeply excavated target material.

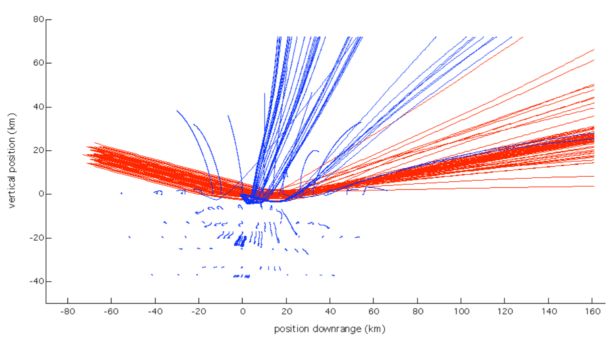

Figure 2: X-Y projection of tracer particle trajectories out to 120 seconds for projectile (red) and target (blue) tracers for the 15˚ run. Excavation of target material is very shallow, very little projectile material is deposited in the crater, and the projectile remains are strongly focussed downrange.

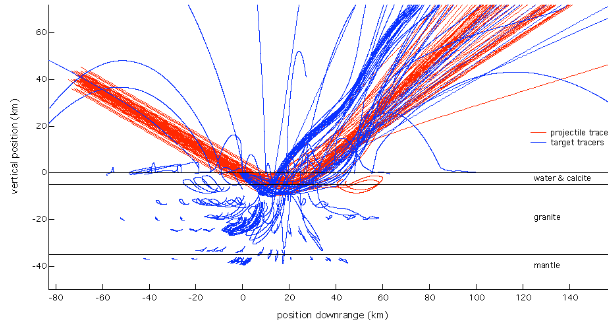

Figure 3: X-Y projection of tracer particle trajectories out to 240 seconds for projectile (red) and target (blue) tracers for the 30˚ run. There is more spreading of both target and projectile material than in the 15˚ run, and some projectile tracers end up buried within the crater. The vertical stratification in the graph indicated here is the same in all model runs.

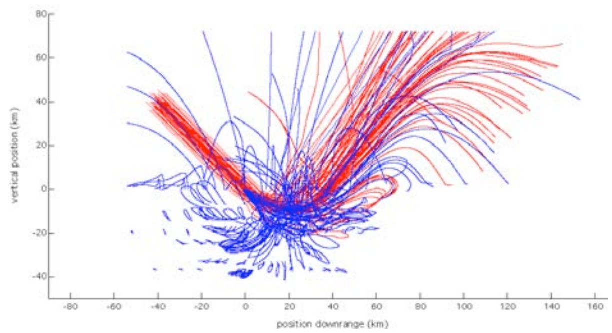

Figure 4: X-Y projection of tracer particle trajectories out to 160 seconds for projectile (red) and target (blue) tracers for the 45˚ run. The ejection of target tracers is more symmetric than in the shallower runs, and a larger proportion of them achieve injection into the stratosphere or into suborbital ballistic trajectories. Still more projectile material is buried within the crater, and more rains back locally than in the shallower impact runs.

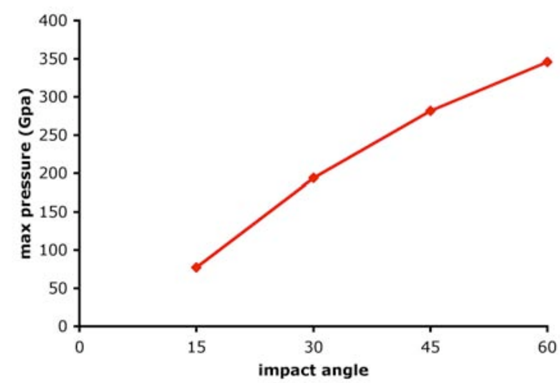

Figure 5: Peak pressures seen at the calcite-granite interface for the 4 runs reported here.